Environment Modeling for Autonomous Welding Robots

Min Y. Kim, Hyung Suck Cho, and Jae-hoon Kim

Abstract: Automation of welding process in shipyard is ultimately necessary, since welding site is spatially enclosed by floors and girders, and therefore welding operators are exposed to hostile working conditions. To solve this problem, a welding robot that can navigate autonomously within the enclosure needs to be developed. To achieve the welding task, the robotic welding system needs a sensor system for the recognition of the working environments and the weld seam tracking, and a specially designed environment recognition strategy. In this paper, a three-dimensional laser vision system is developed based on the optical triangulation technology in order to provide robots with work environmental map. At the same time, a strategy for environmental recognition for welding mobile robot is proposed in order to recognize the work environments efficiently. The design of the sensor system, the algorithm for sensing the structured environment, and the recognition strategy and tactics for sensing the work environment are described and discussed in detail.

Keywords: Autonomous Welding Robot, Laser visual sensor, Environment modeling

I. Introduction

At shipyards, the demands of automatic operations and the desire to pursue a broader automation strategy have fueled the development of new advanced robotic and process control systems. Due to the increase of personnel expenses, the automation of the welding process is necessary for improving the productivity and quality of shipbuilding process. In shipbuilding, a key aspect of the welding process automation is the prefabrication of sub-assemblies on automated lines using robotic welding technology. The welding process for the sub-assembly consists of an open-block welding and an closed-block welding. Many researchers have been doing researches on the robotic welding in shipbuilding. In the case of the open block welding, the gantry welding system [1][2] and a mobile welding robot system [3] has been developed recently and applied to sub-assembly process successfully. However, the research and development for closed-block welding are relatively very few. Recently, due to its necessity this closed-block robot welding system has been drawing a lot of research interests in shipbuilding.

Korea Advanced Institute of Science and Technology (KAIST) and Samsung Heavy Industries Co., Ltd. have developed a mobile welding robot system applicable to the closed-block welding. Fig. 1 shows the interior of the closed block in subassembly to be welded. In manual welding operation, the welding operators pass by floor hole or girder hole during the welding operation. Since the working environment is enclosed with floors and girders, the ventilator must be established for removing the smoke. If this manual welding line is robotized, a feasible work trajectory of the robotic welding system can be illustrated as shown in the figure. When the mobile welding robot completes welding job, it moves to the next block through the floor hole. The environment in which the robot navigates consists of mostly plane structures and their variants. Under this circumstance, it is not an easy task for a robot to navigate through this rather complex environment, to approach the areas to be welded and to find weld seam line accurately. It must be equipped with a capability of sensing and avoiding obstacles to reach the final working zone. For the recognition of the working environment and weld seam lines, a sensor system has been developed which utilizes multi-structured light based on an optical triangulation method [4].

This paper proposes a visual sensing system and a strategy for recognizing the 3D shape of the welding environments. For the recognition of this type of navigating situation and weld seam lines, the sensor system utilizes a multi-structured light based on the optical triangulation method. Based on this perception capability, we presents an environmental recognition strategy for a mobile robot to be applied to closed-block welding in sub-assembly process of shipbuilding. The developed algorithm architecture for efficient environment recognition is composed of a conventional 3D scanning module and a plane generation module utilizing on 3D Hough transform.

The organization of the paper is as follows: In section 2, we introduce the design concept of the welding robot system for closed block assembly. In section 3, the sensor system for seam tracking and welding environment recognition is developed and described in detail. In section 4, the algorithm architecture for environment recognition is described, and a series of experimental tests are performed to verify the efficiency of the proposed sensing system and algorithm. In section 5, a strategy for this environment recognition is proposed, and a series of experimental tests are performed to verify the efficiency of the proposed recognition strategy. Finally, conclusion is made in the last section.

II. Robot tasks for welding closed-block assembly

The mobile welding robot system consists of a welding robot, a mobile platform, and a sensor system. Fig. 2 shows the robot system developed for the closed-block welding process. When the welding robot finishes the welding task within the specified region, the mobile platform must be able to move to next welding space. For this, it can climb across the longi through a specially designed robot mechanism without help of the human operator. After the mobile platform climbs over the longi, then it puts the welding robot down onto the bottom

Manuscript received: Nov. 22, 2000., Accepted: Feb. 25, 2001.
Min Y. Kim, Hyung Suck Cho: Dept. of Mechanical Engineering, KAIST(mykim@lca.kaist.ac.kr/hscho@lca.kaist.ac.kr)
Jae-hoon Kim: Mechatronics Research Department, Samsung Heavy Industries Co., Ltd(kjhcmr@samsung.ac.kr)

plate of the closed block, so that the welding robot moves freely within the space formed between two longis. For environmental recognition tasks, the robot is equipped with a sensor system to be able to perceive and recognize the work environments. Within the free space in the task space between two longis, the operational procedures of the welding robot are as follows:

- welding environment recognition
- matching the acquired 3D map data with the given CAD data
- obstacle detection and avoidance
- welding line detection
- path planning of the robot arms for welding
- robot control and welding

The tasks shown in the above should be performed autonomously by the robot, since no human operator assists any operation to be made. When welding operation is successfully done, the welding robot comes back to the platform waiting during the welding operation. Then, the mobile platform lifts and holds the robot, climbs over the longi and moves to the next task space according to the predefined welding schedule.

III. The sensor system for welding environment recognition and seam tracking

To fulfill the environmental recognition task and welding task, the mobile welding robot is equipped with a sensor system to be able to track the welding seam and to recognize the environments under which it works. In the case of the seam tracking, the optical triangulation method using the structured light has been widely used [5][6], and hence this paper will not treat any topic associated with this.

1. Environmental conditions

Generally, the environmental conditions inside the block are characterized by low intensity of light, dense smog, unpredictable objects, and space structures. If there is no illumination system, the interior of the closed-block is a field of darkness. Despite of ventilation, welding process makes some smog and presents foggy atmosphere. Because the sub-assembly process is the process that welds some pieces of flat plates with different shapes, the working environment under which the robot navigates through can be classified as a structured environment. Due to these reasons mentioned in the above, the developed sensor system must be robust to the lighting condition and smog for accurate 3D recognition of the structured environment.

2. Sensor concept

A variety of machine vision techniques, such as controlled illumination, stereoscopy, photometric stereo, and shape-from-shading has been developed for the determination of 3D scene geometric information from 2D images. However, because of the nature of the manufacturing or welding environment and the type of features of interest, structured lighting is most appropriate and has been widely applied in the sensing tasks mentioned above. In this work, the structured lighting is utilized for environmental sensing.

The sensor system consists of two lipstick cameras and three laser diodes. Fig. 3 shows the concept and the configura

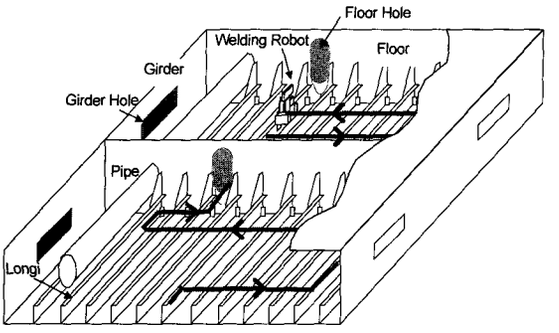

Fig. 1. The interior of a closed-block in sub-assembly and a mobile navigation route.

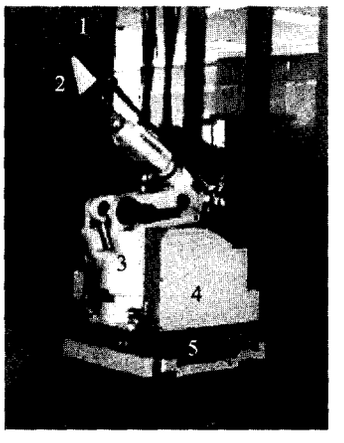

1. welding torch
2. sensor system
3. welding robot
5. mechanism for longi climbing
4. mobile platform

Fig. 2. The mobile welding robot.

tion of the sensor system implemented for detection of the environment in which the mobile welding robot navigates. The first camera (camera A) is used for environmental recognition and the second one (camera B) for weld seam tracking. The first and second lasers (A_1, A_2) are used for environment recognition, and the other (B) is for seam tracking. The two laser stripes make the recognition of the structured environment easy. The detailed description is presented in reference [4].

3. Image processing algorithms

The imaging processing algorithm is to extract laser stripe data from acquired images which may contained other possible brightness source such as the reflection of laser light from the unknown specular object, and welding glares.

To perform laser stripe extraction robustly, it needs to discriminate the laser stripe distinctly from noise sources.

The most reliable feature for extracting laser stripe is thickness of laser stripe in the image plane. The basic idea of robust extraction of laser stripe is to find the highlighted line which has a known thickness of laser stripe in an acquired image. For laser stripe extraction, Kim and Cho[6] proposed a spatial filter which yields maximum response to the center of the laser stripe through the convolution with the original pixel data. In this study, however, the thickness of laser stripe is

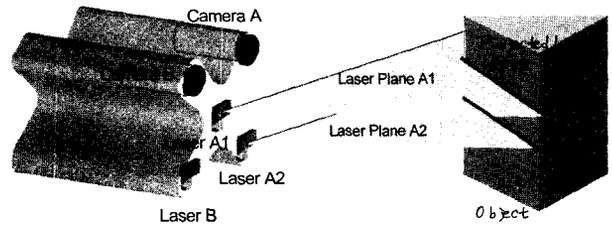

(a) The concept of the sensor system

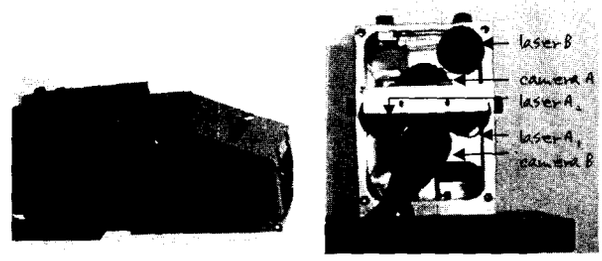

(b) The configuration of the implemented sensor system

Fig. 3. The visual laser sensor system.

slightly changed depending on the distance from target object to laser source or the stripe location on image plane. In the basic experiments using the developed sensor system, the difference of laser thickness between image center and image corner is found to be about 13 pixels where the laser source is 0.5~1m far from target object. The image in the corner is slightly blurred, thus, the thickness change of laser stripe occurs because the focal depth of camera lens in the vision system has a little limitation to cover the whole range between camera and objects.

For this reason, it is difficult to find only one spatial filter for yielding maximum response to the center of the laser stripes with various thickness in an image. To overcome the above mentioned problem, a neural network-based multi-spatial filter techniques is proposed. The basic idea of the neural approach is that the neural network can learn the center of laser stripe from various thickness of laser stripe. The structure of the proposed neural network is shown in Fig. 4. The neural network used here is a multi-layer perceptron and consists of an input layer and 2 hidden layers and an output layer. Input layer has 35 neurons and each hidden layer 20 and 10 neurons, respectively. The inputs of neural network are the graylevel value of each vertical pixel on laser stripe and the image coordinates (u,v) of the center position of input window, A. Its output is the probability of the center of laser stripe, $P_{line\ center}$. When neural network mask lies in the center of laser stripe, the probability of the line center, $P_{line\ center}$, yeilds the maxi-mum probability near to 1. During the learning phase of the neural network, the input data sets of vertical profile of laser stripe and pixel coordinates of the center of the searching window are provided to learn various laser thickness in the image plane. After learning phase, the neural network spatial filter is able to estimate thickness of the stripe and to calculate the center line of the laser stripe.

To extract the line center of laser stripe, the neural spatial filter operates in the direction of column of the images, because the stripe is approximately parallel to the rows of the image. For the weight training of the multiplayer neural network, the modified back propagation method is applied with learning-rate adaptation called *delta-bar-delta learning rule*[10]. Let $w_{ji}(n)$ denote the value of the synaptic weight connecting neuron i to neuron j, at iteration n. Let $\eta_{ji}(n)$ denote the learning-rate parameter assigned to the weight update mechanism at this iteration. The learning-rate update rule is defined as follows:

$$\Delta\eta_{ji}(n+1)=\begin{cases}\kappa & \text{if } S_{ji}(n-1)D_{ji}(n)>0\\ -\beta\eta_{ji}(n) & \text{if } S_{ji}(n-1)D_{ji}(n)<0\\ 0 & \text{otherwise}\end{cases} \tag{1}$$

where $D_{ji}(n)$ and $S_{ji}(n)$ are defined as, respectively

$$D_{ji}(n)=\frac{\partial E(n)}{\partial w_{ji}(n)} \tag{2}$$

and

$$S_{ji}(n)=(1-\xi)D_{ji}(n-1)+\xi S_{ji}(n-1) \tag{3}$$

where ξ is a positive constant, κ and β are the control parameters, and E(n) is the cost function as the instantaneous sum of squared errors,

$$E(n)=\frac{1}{2}\sum_{j}[d_j(n)-y_j(n)]^2 \tag{4}$$

where $y_j(n)$ is the response of the output neuron j, and $d_j(n)$ is the desired response for that neuron. The update formula for the jith synaptic weight as

$$w_{ji}(n)=w_{ji}(n-1)-\eta_{ji}(n)\frac{\partial E(n-1)}{\partial w_{ji}(n-1)} \tag{5}$$

Fig. 5 shows the line extraction results of an acquired image with laser thickness variation, and the proposed method compared with the conventional method gives more robust result for the test image.

4. Calibration and resolution analysis

Since the structured lighting approach using a plane of light is relatively well known, only an overview of the calibration methodology is presented here for completeness. Fig. 6 (a) shows the concept of sensor calibration. The fixed coordinates

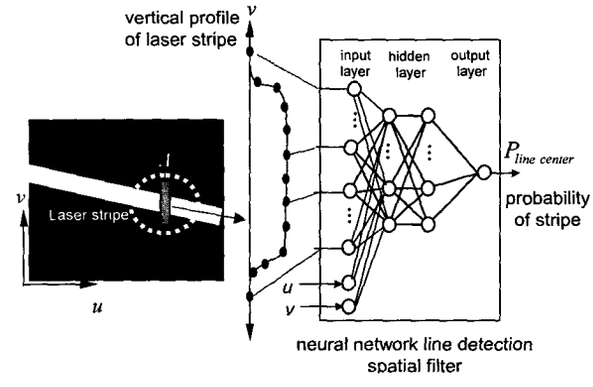

Fig. 4. Neural network structure for line extraction.

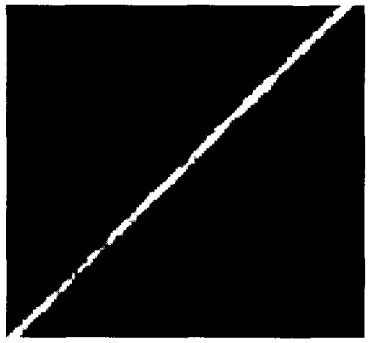

(a) Laser stripe with the variation of thickness

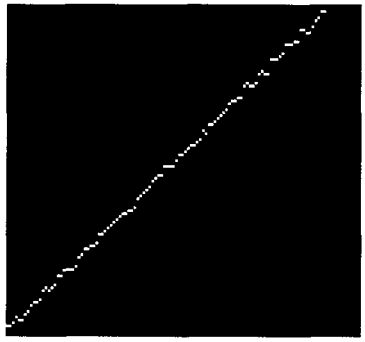

(b) Conventional method[6]

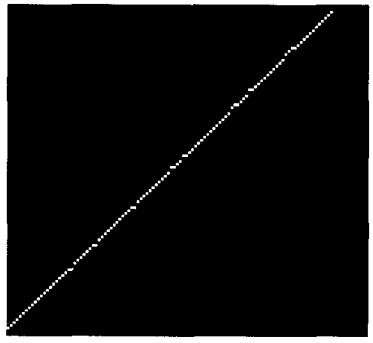

(c) Proposed method

Fig. 5. The line extraction.

$OXYZ$ are denoted as the world coordinates, the 2D coordinates uv denote the pixel coordinates on image plane, and the $X'Y'$ is defined as the image plane coordinates. Specifically, to compute the 3D coordinates (x, y, z) of any point on the laser strip from the 2D coordinates (u, v) of its image, a transformation T (4x3 matrix) relating the world and image homogeneous coordinates in the form

$$s[x, y, z, 1]^T = M[u, v, 1]^T \tag{6}$$

is needed, where s is the scaling factor of the homogeneous transform and M is the perspective transformation matrix. This transformation can be computed off-line during the camera and laser projector calibration phase by observing the feature point in image and the laser stripes on an accurately machined block gauge of known dimensions (Fig. 6).

On implementation of 3-D measurement system, the most important variable is the measurement resolution. In the measurement system using laser slit-ray, the resolution is defined as lateral resolution (X and Y direction) and vertical resolution (Z direction). In Figs. 7 and 8, the diagrams for resolution analysis are presented on projective planes (XZ, YZ, and XY plane). Here, the L_X and L_{Y1} are the vertical and horizontal field of view of the camera at depth T, respectively. T is denoted as the maximum measuring distance in Z direction, which θ denotes the separation angle of laser slit beam, and f is the focal length of the camera lens. The Z axis coincides with the camera's optical axis, and the distance D denotes base line between camera and laser diode. α and β are the field angles of camera view on Y' and X' plane, respectively. At depth z, a and b are the vertical and horizontal pixel length due to one pixel on image plane. If we let $P'(x',y')$ be the projective point on image plane of $P(x, y, z)$ in 3-D space, then, the angles between a line OP' and z axis are denoted as ϕ and ψ on XZ and YZ plane, respectively. M_{X2} is the distance from the optical axis in X direction at the maximum measuring distance, and M_{X1} the minimum measuring distance. M_Z is denoted by the measuring range of this sensor system in Z direction.

From the geometric relations shown in Figs. 11 and 12, we can obtain the resolution of the optical triangulation based sensor system in each axis as follows:

$$R_X = \frac{2p_{x'}f(2T - L_X \tan\theta)}{[2f - 2(x' + p_{x'})\tan\theta](2f - 2x'\tan\theta)} \tag{7-1}$$

$$R_Z = \frac{2p_{x'}f\tan\theta(2T - L_X \tan\theta)}{[2f - 2(x' + p_{x'})\tan\theta](2f - 2x'\tan\theta)} \tag{7-2}$$

$$R_Y = \frac{L_{Y1}}{l_v T} \cdot \frac{f(2T - L_X \tan\theta)}{2f - 2x'\tan\theta} \tag{7-3}$$

where l_u and l_v are the total vertical and horizontal pixel number of CCD, respectively, and L_{Y1} and L_{Y2} denote the maximum and minimum measuring range in Y direction. The effective pixel size $p_{x'}$ and $p_{y'}$ are then expressed by

$$p_{x'} = l_{x'} / l_u \tag{8-1}$$

$$p_{y'} = l_{y'} / l_v \tag{8-2}$$

where $l_{x'}$ and $l_{y'}$ are the vertical and horizontal size of the effective area of CCD chip, respectively.

To design a proper sensor system, the resolution variation in each axis was observed through a series of computer simulations. The derivation of the resolution equations and the simulation results are described in detail in reference [4]. In case of the implemented sensor system, the seperation angle θ of the environmental recognition sensor part is about 75°. Table 1 shows the results of the resolution analysys of this sensor part.

Table 1. Resolution analysis for the environmental recognition sensor system. (Unit: mm)

Distance	R_Z	R_X	R_Y
600	2.4	0.3	0.2
1000	3.5	0.6	0.3
1400	4.9	1.0	0.5
1800	6.5	1.7	0.7

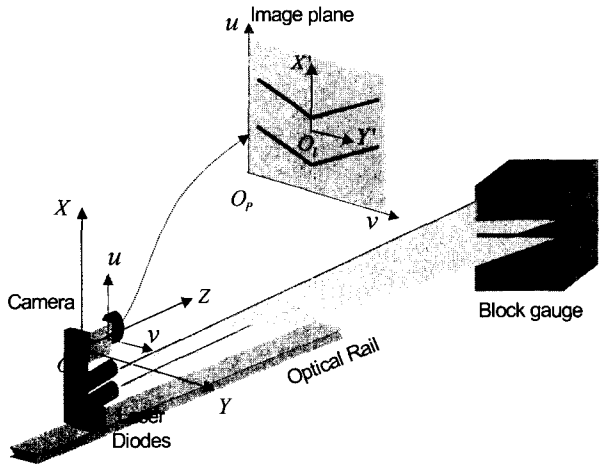

(a) Conceptual diagram

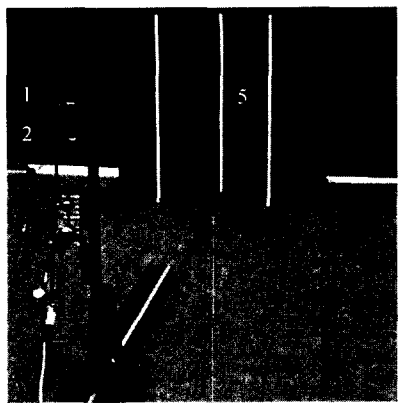

1. laser diode 1 2. laser diode 2
3. CCD camera 4. optical rail
5. block gauge

(b) Experimental set-up

Fig. 6. Sensor system calibration.

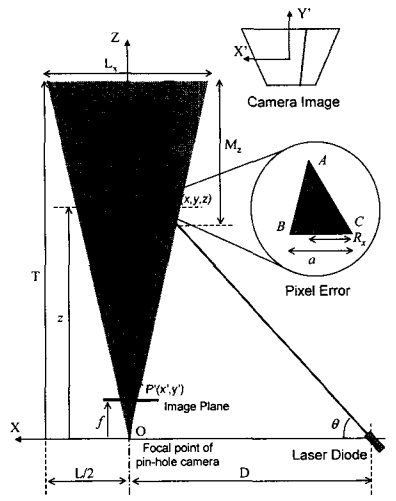

Fig. 7. Resolution analysis on XZ plane.

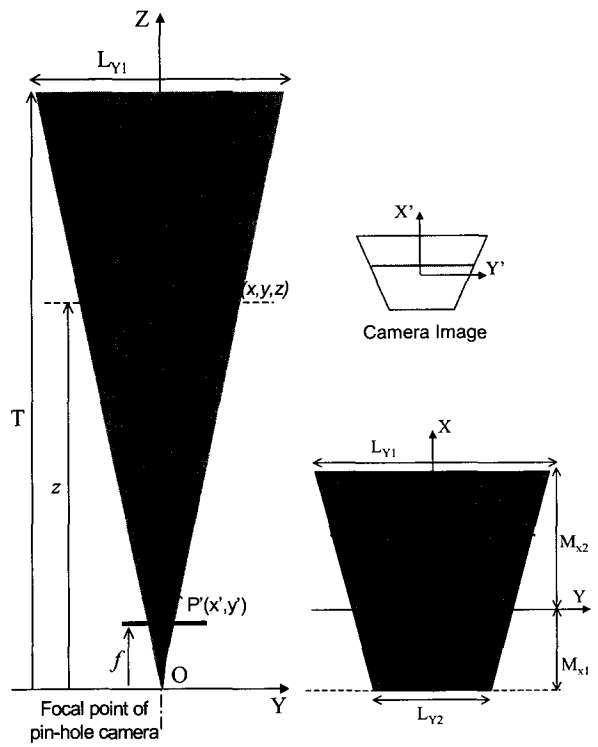

(a) Planar YZ view (b) Planar XY view

Fig. 8. Resolution analysis on YZ plane.

IV. Construction of the environment

1. The plane generation method

The interior of the close-block is essentially a structured environment composed of several planes with different shapes. When two laser stripes are projected on a plane, two straight-lines appear in image plane as shown in Fig. 6 (a). Generally, the line equation in 3D spaces is as follows:

$$\vec{x} = \vec{a} + t \cdot \vec{b} \tag{9}$$

where $\vec{a}$ is the positional vector and $\vec{b}$ is the directional vector of the line. Two straight lines in image plane can be detected by Hough transform [7]. Using the acquired line equation in 2D image plane and Eq. (6), the 3D line equation can be acquired easily. Fig. 9 shows the plane generated from two lines. Let the acquired 3D line equations be L_1 and L_2. From Eq. (9), these lines are represented as follows:

$$L_1: \quad \vec{x} = \vec{g}_1 + t \cdot \vec{h}_1 \tag{10a}$$

$$L_2: \quad \vec{x} = \vec{g}_2 + t \cdot \vec{h}_2 \tag{10b}$$

where the $\vec{h}_1$ and $\vec{h}_2$ denote the directional vectors of the line L_1 and the L_2, respectively, and the $\vec{g}_1$ and $\vec{g}_2$ the positional vectors of the lines. Generally, the plane equation in 3D spaces and its vector form are given by:

$$\vec{x} \cdot \vec{k} - d = 0 \tag{11}$$

where $\vec{k}$ is normal vector of the plane and d is the distance from origin to the plane. In the case that the L_1 and L_2 lie on the plane P_1, the directional vector $\vec{h}_1$ of the line L_1 and the $\vec{h}_2$ of the L_2 make the normal vector $\vec{k}$ of the plane P_1 by the equation

$$\vec{k} = \vec{h}_1 \times \vec{h}_2 . \tag{12}$$

If Eq. (12) is substituted to Eq. (11), d can be calculated without difficulty.

2. Experimental results

To observe the utility of the plane generation method, a series of experimental tests are performed. Fig. 10 shows a folded plate used for this test. With a variation of a folding angle θ, the plane generations using two laser stripes are tested. By use of the proposed method, four geometrical parameters in the plane equation are determined and compared with the real values. Table 2 and Fig. 11 present the experimental results. The experimental results show that the maximum ranges within ±2% error. The main aspect of these errors is due to the misalignment of the laser stripes, the calibration error, the positioning error of the object, and others. In case of θ = 45°, the measured data and real data on YZ plane is shown in Fig. 11, and the maximum error is about 8mm. Based on the acquired plane parameters, the test plate can be reconstructed in virtual space as shown in Fig.12.

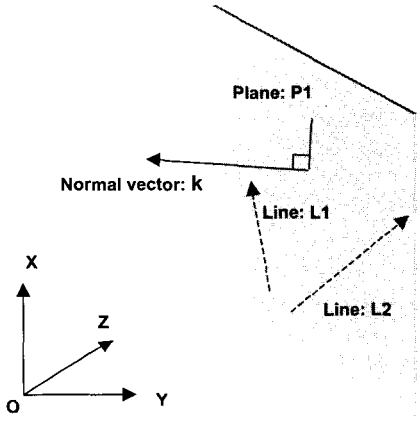

Fig. 9. Plane constructed from the two lines.

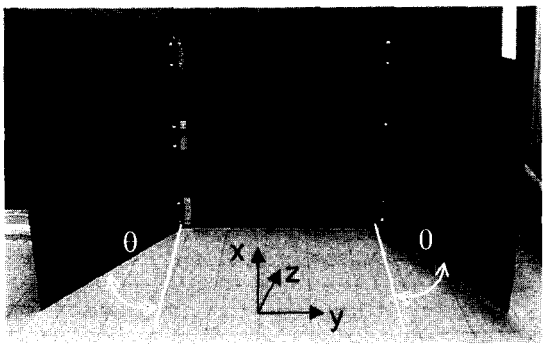

Fig. 10. Folded plate for experimental tests.

Table 2. Experimental results for the plane generation.

θ		k_1	k_2	k_3	$d(m)$
22.5°	real	0.000	-0.923	-0.382	0.382
	measure	0.003	-0.921	-0.395	0.375
45°	real	0.000	-0.707	-0.707	0.707
	measure	-0.002	-0.713	-0.705	0.709
67.5°	real	0.000	-0.382	-0.923	0.923
	measure	0.002	-0.368	-0.921	0.928

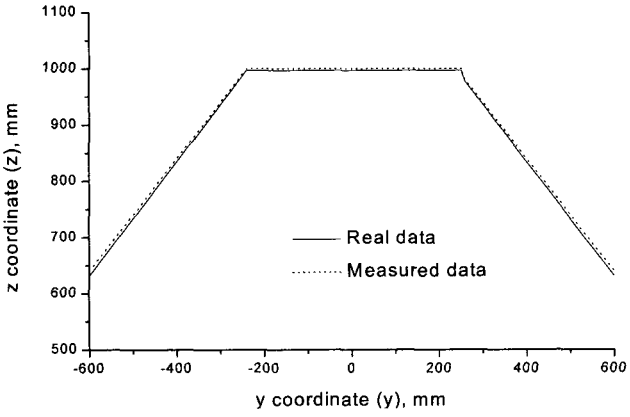

Fig.11. Experimental result in case of θ= 45°(YZ Plane).

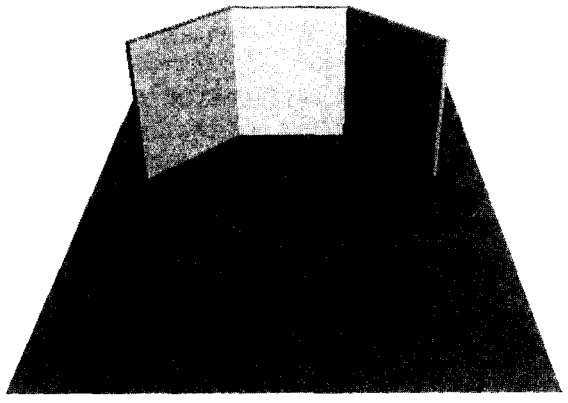

Fig. 12. Reconstructed test plate in virtual space.

V. Strategies of the environment recognition

1. Field definition and data representation

The task space formed between two longis is classified into three subspaces; far field, middle field, and near field according to the robot-to-welding environment distance. The strategy for the welding environment recognition is defined at each field as shown in Fig. 13. The range of each field is limited to the working range of the sensor. The algorithm architecture for the environment recognition is divided into two parts. The first is the conventional 3D scanning module, and the second the plane generation module utilizing Hough transform. These modules are appropriately selected at each task. The detailed description for the tasks in each field is presented in next section.

Many different environment representations can be used according to the type of task to be performed, the kind of environment, and the type of sensor used. The most significant types of representations are cell decomposition models, geometrical models and topological models [8]. In this work, we select the cell decomposition modeling technique as an object representation method. This technique is not able to represent an object to be modeled exactly. However, any object can be represented in a simple way by this method. Fig. 14 shows the cubic cells with 100x100x100 size for 3D environment models. The one cubic cell (voxel) has 10x10x10mm volumetric size. This volumetric size was determined on considering the sensor resolution analysis result in section 4.

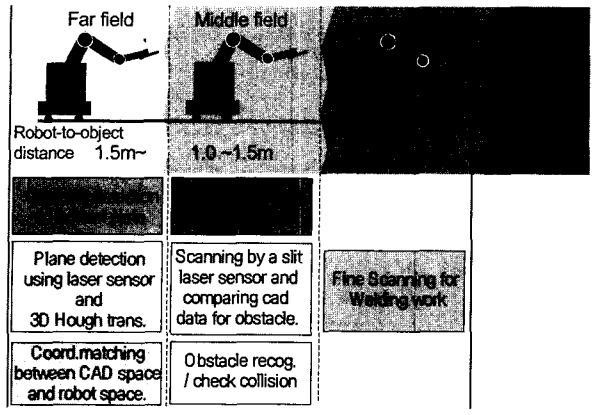

Fig. 13. Measuring field definition and tasks at each field.

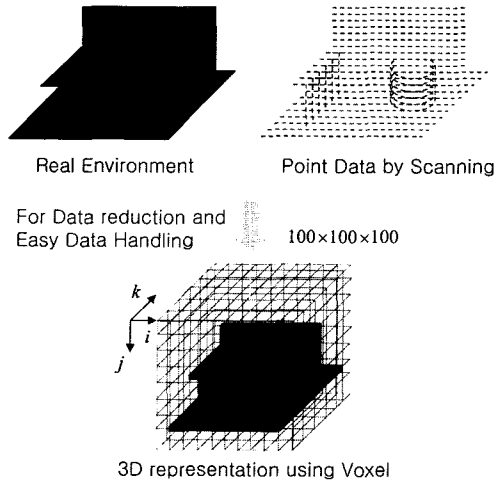

Fig. 14. Cubic cells for a 3D environment model.

2. Far field

The mobile robot tasks in the far field are mainly decomposed into three subtasks:

task 1: detection of obstacles on bottom plate

task 2: plane detection using 3D Hough transform

task 3: coordinates matching between CAD space and robot space

In task 1, 3D scanning task is executed using one laser stripe sensor to detect the obstacles on bottom plate. In task 2, planes are detected via the plane generation module using the measured data obtained from two laser stripes. When the robot settles down in a new task space between tow longis, it needs localization in world coordinates frame. For this purpose, we propose a positioning method using the plane detection. Fig. 15 shows the plane recognition using two laser stripes described in section 4. When the two laser stripes are projected on a plane, the plane equation can be derived from the 3D line equations of the stripes observed on an image plane. For the robot localization, the planes to be recognized are a floor, two longis, and a bottom plate. In task 3, a coordinate matching task is carried out for the localization. The coordinate transform matrix between robot coordinates and world coordinates can be acquired by matching the detected planes into the CAD plane data. This matching technique used here is based on the least square error method [9]. Fig. 16 shows the concept of the plane matching for transformation of robot coordinates and world coordinates.

Using the acquired transform matrix, the measuring data on objects in the environment in the robot coordinate frame can be transformed into and expressed in world coordinate frame.

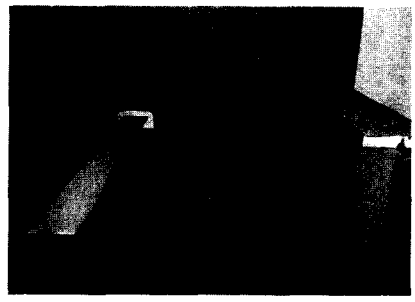

(a) Two laser stripes projected on a real environment

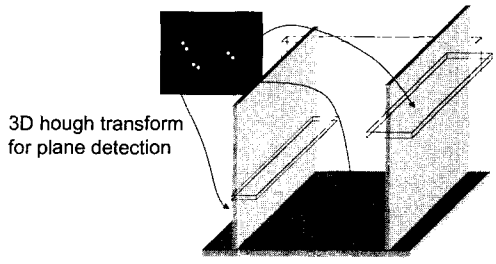

(b) Plane detection using 3D hough transform

Fig. 15. Plane recognition using two laser stripes.

3. Middle and near fields

The tasks in the middle field are divided into three major subtasks:

task 1: detection of obstacles on side plates (longi)

task 2: scanning by a single slit laser sensor and comparing CAD data for obstacle detection

task 3: obstacle recognition and collision check of robot arm

The task carried out in the near field is to finely scan around the obstacle region defined in middle field.

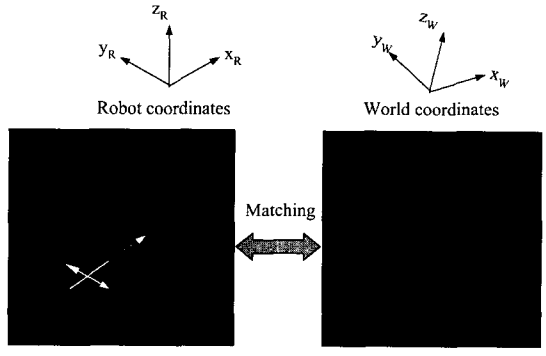

(a) The detected planes (b) CAD data

Fig. 16. Plane matching for transformation of robot coordinates and world coordinates.

In order that the robot can access from the far field to the

middle field, it is necessary to detect obstacles on side walls first. To carry out all tasks associated with the middle and near fields, the scanning module in algorithm architecture is utilized. Fig. 17 shows the concept and a typical experimental result of detection of an obstacle on side plane(wall). The detailed description on comparing two data for the obstacle detection is presented in reference[11]. Fig. 18 shows the scanning results obtained from the environment composed of a cylinder and a cubic in the middle and near fields.

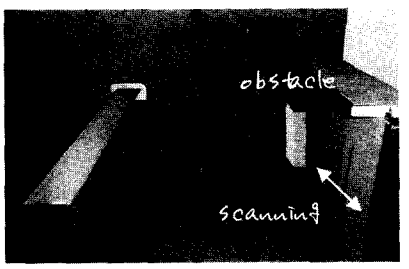

(a) A laser stripe projected onto a real environment

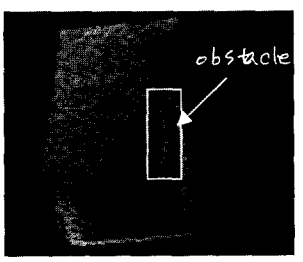

(b) The obstacle detected by scanning

Fig. 17. The detection of a obstacle on side plate.

VI. Conclusions and further works

In this paper, we have considered an autonomous mobile robot that can navigate within a specified indoor environment of a shipbuilding. To achieve the autonomous robot navigation and robotic welding, we developed a sensory system using three laser stripes and two CCD cameras which detects the welding locations and recognizes the 3D shape of the welding environments. Through the sensor resolution analysis, the developed sensor system was designed to have about 4mm depth resolution at 1m object distance for the environment recognition.

Based on this perception capability, we presented an environmental recognition strategy for a mobile robot to be applied to closed-block welding in sub-assembly process of shipbuilding. For the efficient recognition of welding environment, the developed algorithm architecture is composed of the conventional 3D scanning module and the plane generation module utilizing 3D Hough transform. Through the experimental tests, the utility of the proposed plane generation method was evaluated. The evaluation results show a good applicability of this method for recognition of the structured environment within 2% parameter estimation error. Finally, the strategy for the welding environment recognition was proposed at far field, middle field, and near field with some application results, and the basic evaluation experiments for the proposed strategy were performed.

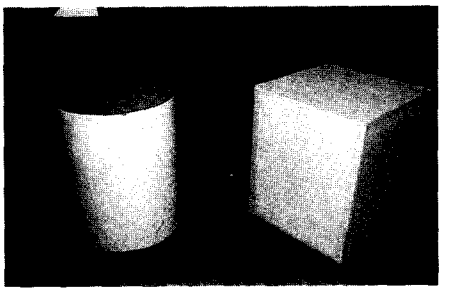

(a) A real environment

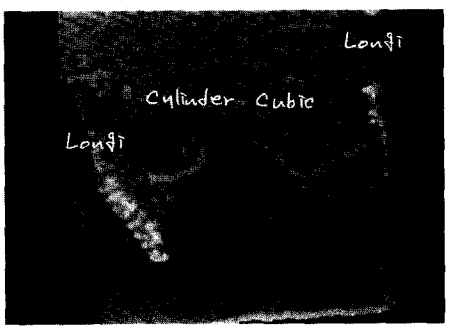

(b) The scanning data represented in voxel space

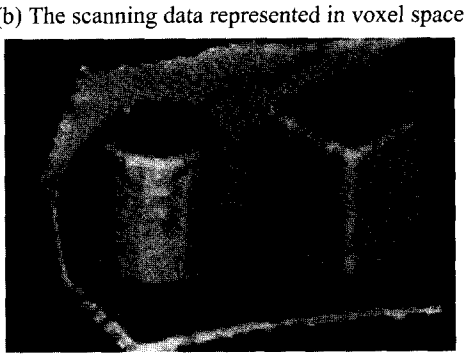

(c) The fine scanning result in the near field

Fig. 18. The scanning results for the real environment.

Now, we are performing the recognition tests for the objects with the more complex shapes. The development of this robotic system is still under way. Following issues can be summarized as further works:

- Development and extension of the environment recognition algorithms
- Extraction of the obstacle information from the 3D environment data
- Geometrical modeling of each obstacle.

References

[1] D. M. Wihsbeck, "Application update: robotized welding in shipbuilding-installation, off-line programming, experiences," *Proceedings ICARCV*, pp. 10-14, 1998.

[2] P. Sorenti, "Efficient robotic welding for shipyards-virtual reality simulation holds the key," *Industrial Robot*, vol. 24, no. 4, pp. 278-281, 1997.

[3] Hitachi, *HYROBO manual*, Hitachi, 1993.

[4] M. Y. Kim, K. W. Ko, H. S. Cho, and J.H. Kim, "Visual sensing and recognition of welding environment for intelligent shipyard welding robots," *Proceedings of IEEE/RSJ IROS 2000*, pp. 2159-2165, 2000.

[5] B. Bahr, J. T. Hqung, and K. F. Ehmann, "Sensory guidance of seam tracking robots," *Journal of Robotic Systems*, vol. 11, no. 1, pp. 67-76, 1994.

[6] J.S. Kim and H.S. Cho, "A robust visual seam tracking system for robotic arc welding," *Mechatronics*, vol. 6, no. 2, pp. 141-163, 1996.

[7] D. H. Ballard and C. M. Brown, *Computer vision*, Prentice Hall, 1982.

[8] M. A. Salichs and L. Moreno, "Navigation of mobile robots: open questions," *Robotica*, vol. 18, no. 3, pp. 227-234, 2000.

[9] Z. Zhang, "Parameter estimation techniques: a tutorial with application to conic fitting," *INRIA Technical Report*, no. 2676,1995.

[10] S. Haykin, Neural Networks: A Comprehensive Foundation, *Macmillan*, 1994.

[11] M. Y. Kim, H. S. Cho, and J.H. Kim, "Neural network-based recognition of navigation environment for intelligent shipyard welding robots," *Submitted to IEEE/RSJ IROS 2001*, 2001.

Min Young Kim

He was received his B.S. degree and M.S. degree from Korea Advanced Institute of Science and Technology (KAIST), Korea in 1996 and 1998, respectively. He is currently a Ph.D. student at the same institute, studying on 3D environment recognition. Current interests of research include 3D machine vision and its robot application, neural networks and environment modeling.

Jae-hoon Kim

He received his BS degree in mechanical engineering from Seoul National University, Korea in 1980, his MS degree in systems engineering from Wright State University, Dayton, Ohio in 1985, and his Ph.D. degree in aerospace engineering from Purdue University, West Lafayette, Indiana in 1991. From 1979 to 1987 he was a researcher with Agency for Defence Development, Korea. From 1984 to 1985 he was an exchange engineer with USAF Flight Dynamics Laboratory at Wright Patters on Air Force Base, Dayton, Ohio. Since 1992 he has been a principal researcher with Samsung Heavy Ind-ustries, Co. Ltd. His research interests include structure/control interaction, sensor/actuator selection, autonomous mobile robot, robot application and welding automation.

Hyung Suck Cho

He was received his B.S. degree from Seoul National University, Korea in 1971, his M.S. degree from Northwestern University in 1973, Evanston, IL, USA. and his Ph.D. degree from the University of California at Berkeley, CA,USA. in 1977. From 1977 to 1978 he was a postdoctoral fellow with the Department of Mechanical Engineering, University of California at Berkeley. Since 1978 he has been a professor with Department of Production Engineering, Department of Automation and Design, Seoul Campus, and currently with Department of Mechanical Engineering, Korea Advanced Institute of Science and Technology(KAIST), Korea. His research interests are focused on the area of environment perception and recognition for mobile robots, machine vision and pattern classification, and application of artificial intelligence/machine intelligence. Now, he serves on editorial boards of international journals, Journal of Robotic Systems, Robotica, Control Engineering Practice (IFAC), Journal of Advanced Robotics and Journal of Engineering Manufacture (PIME). In 1998 he served as a guest editor on a special issue on "Intelligent Robotic Assembly" for the journal, Robotic